PAPER Nr. : 68

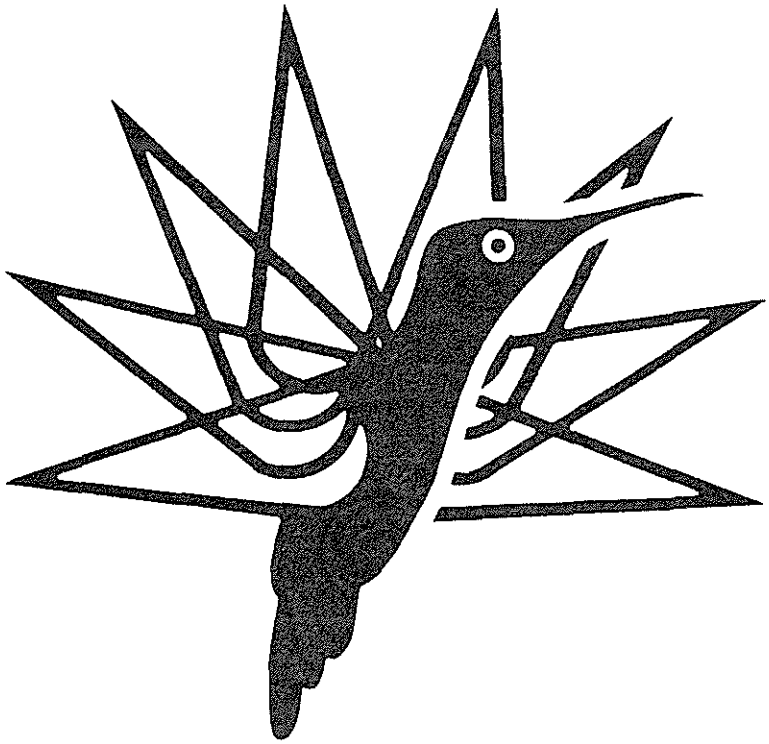

IDENTIFICATION OF ROTOR DYNAMIC EFFECTS IN FLIGHT DATA

BY

J. BLACKWELL, R.A. FEIK, AND R.H. PERRIN

AERONAUTICAL RESEARCH LABORATORY
P.O. BOX 4331, MELBOURNE 3001, AUSTRALIA

FIFTEENTH EUROPEAN ROTORCRAFT FORUM

SEPTEMBER 12 - 15, 1989 AMSTERDAM

IDENTIFICATION OF ROTOR DYNAMIC EFFECTS IN FLIGHT DATA

J. Blackwell, R.A. Feik, and R.H. Perrin
Aeronautical Research Laboratory
P.O. Box 4331, Melbourne 3001, Australia

ABSTRACT

In a recent investigation of Sea King vertical motion characteristics in response to collective inputs in hover, it was shown that modelling of blade flapping and rotor speed dynamics as well as dynamic inflow effects was essential in order to match predictions with flight measurements.

The inclusion of rotor speed effects raises the question of blade lagging dynamics which are generally regarded as unimportant in relation to flying quality characteristics. However, there is reason to believe that blade lagging dynamics needs to be represented in order to achieve a consistent set of rotor speed parameters in the identified vertical response model for the Sea King. The inclusion of blade lagging also leads to a closer match with measured rotor speed changes when larger collective inputs are applied.

Currently, work is being directed towards modelling dynamic response characteristics to cyclic inputs, both in hover and in forward flight. In this case rotor speed changes are small and can be neglected, but the equations are complicated by the need to model coupling between longitudinal and lateral blade flapping. The dynamic inflow equations are also more complex. A simple alternative which has been suggested involves the representation of rotor flapping dynamic effects by time shifts in the cross axis response characteristics. Both modelling approaches are being used, with particular interest focussed on a comparison between the respective model parameters which are identified. Time domain parameter estimation techniques are used to match model predictions with flight measurements for a Sea King helicopter. Extracted parameters include those representing aerodynamics, blade flapping and inflow dynamics, and time shifts. Although linearised small disturbance models are generally used, the identification technique is applicable to general non-linear systems.

This paper will briefly review previous results on Sea King vertical response dynamics and present some new results on the effect of blade lag dynamics on rotor speed response. The results of the present work on cyclic response characteristics will also be presented. In particular this will include a comparison of results obtained from a simple time shift model and a model which represents blade flapping and inflow dynamics. Identified parameter values and time history matches will be used in assessing their relative merits.

1. INTRODUCTION

Rotorcraft flight dynamics is characterised by the coupled nature of helicopter motions, making it difficult to separate out the degrees of freedom except in special cases. Inclusion of rotor dynamic effects such as blade flapping and lagging, inflow variations, and rotor speed changes, can lead to a large model of considerable complexity in the general case. Simplified models may neglect rotor dynamic effects entirely or attempt to account for higher order effects by the use of a time delay. The success of such approximations depends on the intended application of the model. In order to increase understanding of which features it is important to retain, it is useful to isolate areas of interest where modelling deficiencies are apparent, and focus on the the development of adequate model structures which can be verified more readily than a large complex general purpose model. For the present investigation the examples chosen have been restricted to hovering flight in order to focus on some particular aspects of interest.

In Reference 1, a six degree of freedom rigid body model was used to model a Sea King Mk 50 helicopter, and validations carried out by comparisons against flight trials data. While such a modelling approach provided a reasonable representation of performance and flight dynamic characteristics over a range of airspeeds, some noticeable deficiencies were obvious. In particular, the vertical acceleration transient response characteristics to collective step inputs were poorly predicted, and roll cross coupling response with longitudinal cyclic inputs indicated a phase shift which was not correctly modelled. Both of these phenomena have significant flying qualities implications and accurate representation would be important in simulators and for applications such as stability augmentation system design.

A recent investigation of the vertical response characteristics in hover (Reference 2) showed that modelling of blade flapping and rotor speed dynamics as well as inflow dynamics was essential in order to match predictions with flight measurements. However, some remaining discrepancies in the rotor speed time history match, and inconsistencies in the rotor speed parameters suggested that blade lagging

may need to be considered to obtain a model with good predictive qualities over a range of flight conditions and manoeuvres. For responses to cyclic inputs, rotor speed changes are not important, but coupling between pitch and roll motion is a characteristic feature in which blade flapping and inflow dynamics can be assumed to play a role. The adequacy of using an equivalent time delay to approximate these effects is also of some interest.

Parameter estimation techniques have been extensively used to determine fixed wing aircraft flight parameters from flight test data (Reference 3) and are finding wider application in the rotorcraft community. As shown in Reference 2, they provide a useful tool for developing adequate model structures and for extracting estimates for the corresponding parameters. For non-linear systems, a time domain approach has been developed at the Aeronautical Research Laboratory (ARL) which provides the necessary flexibility for making rapid model changes and estimating non-linear parameters including time delays (Reference 4).

In the next section, particular modelling deficiencies will be illustrated using the Sea King flight data, followed by a brief description of the parameter estimation methodology used here. The vertical response dynamics model will then be reviewed and some new results presented on the effect of blade lagging dynamics on rotor speed response. Finally recent work on developing a cyclic response model will be described including a comparison of results obtained from a simple time shift model and models which successively incorporate blade flapping and inflow dynamics.

2. FLIGHT DATA

The Sea King Mk. 50 helicopter has a fully articulated main rotor of five blades, and a conventional tail rotor of six blades. Propulsion is by twin, free turbine Rolls-Royce H1400-1 Gnome engines. The basic layout is shown in Figure 1. A flight test program provided a comprehensive data base for both performance and flight dynamics characteristics. Measured data included control inputs from which blade angles were derived, and a full complement of body attitudes, rates, and c.g. accelerations, together with engine torque and rotor speed. Air data from a nose boom unit were also measured but no instrumentation was provided on the blades. The data were recorded in 12 bit form at a sampling rate of 60 Hz and subject to a range of post-processing procedures to reduce random noise levels, correct various error sources such as "drop-outs" and known time delays, and to ensure kinematic consistency.

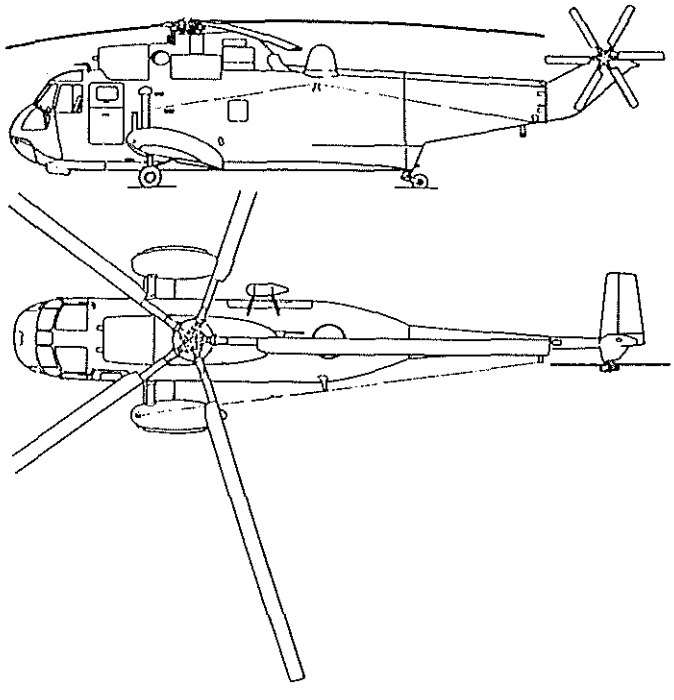

Figure 1 - Sea King Mk 50 General Arrangement

A comparison between mathematical model predictions and flight data was reported in Reference 1, The model consisted of six degrees of freedom rigid body dynamics and a simple representation of rotor speed changes, but blade or inflow dynamics were not included. The results indicated adequate agreement between predictions and measurements over a range of conditions but noted particular areas of discrepancy in transient response characteristics to step and pulse control inputs. Unfortunately other input types such as doublets, 3211 multisteps, or frequency sweeps were not included in the tests.

Two major areas of discrepancy are illustrated in Figures 2 and 3, both for hovering flight. In the former, vertical acceleration and rotor speed response to a collective step shows the poor agreement achieved in both the initial acceleration peak and in the longer term oscillatory characteristics. Figure 3 shows an example of dynamic pitch and roll response to a longitudinal cyclic pulse input. Although the primary pitch rate appears to be predicted reasonably well there is a large phase shift in the roll response.

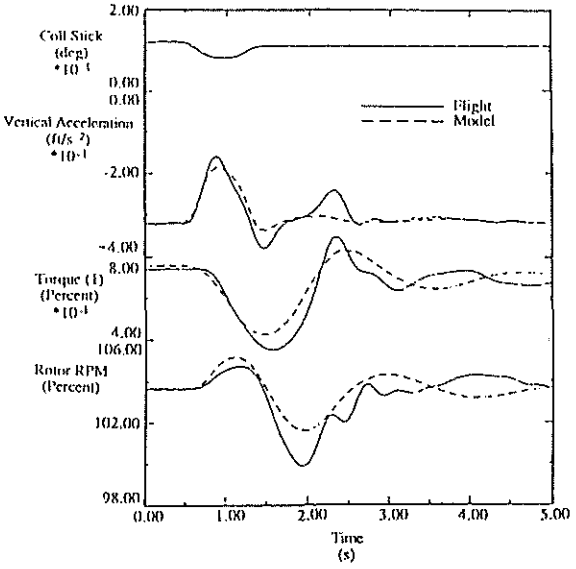

Figure 2 - Response to Collective Pulse in Hover

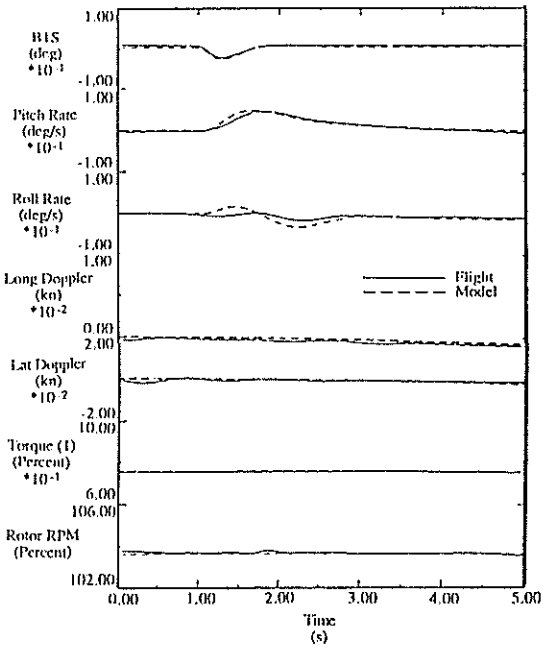

Figure 3 - Response to Longitudinal Cyclic Pulse in Hover

3. PARAMETER ESTIMATION METHODOLOGY

A time domain maximum likelihood program applicable to general non-linear systems has been used to investigate the model deficiencies described in the previous section. Details of the method are described in standard references (e.g. Reference 3) and amount to the minimisation of a cost functional which is the weighted sum of output errors. A modified Newton-Raphson algorithm is used to achieve the minimisation iteratively. The principal computational burden is associated with the calculation of the sensitivity matrix whose jk^{th} element is the partial derivative of the j^{th} output with respect to the k^{th} parameter, $\frac{\partial y_j}{\partial \xi_k}$.

The ARL program uses numerical differences to approximate the sensitivity matrix elements:

$$\frac{\partial y_j}{\partial \xi_k} = \frac{y_j(\xi_k + \Delta\xi_k) - y_j(\xi_k)}{\Delta\xi_k} \qquad (1)$$

This means that explicit sensitivity equations are not required so that non-linear type parameters, such as discontinuities and time delays, can be readily estimated. Considerable flexibility in making model changes is also provided. The ARL program is described in more detail in Reference 4. The

Cramer - Rao lower bound which is also computed provides an estimate of parameter relative accuracy, although it is recognised that, as an absolute measure, it significantly over-estimates that accuracy.

When rotor dynamics effects are included, candidate mathematical models can contain a large number of unknown parameters. Reliable estimates of all parameters is not possible because of the limitations in the information available (e.g. no blade flapping or lagging measurements) and the non-optimal input shapes used. In addition many of the parameters are closely related, and not really independent. The latter problem can be avoided by imposing constraints on appropriate parameters based on a priori expressions from the derived model. Further, an order of magnitude analysis can be used to fix the less significant parameters at their a priori values. By this means, the number of unknown parameters can be reduced sufficiently to enable convergence of the algorithm to be achieved and reliable parameter estimates to be extracted in most cases.

4. COLLECTIVE RESPONSE

4.1 Background

In Reference 2, a model which provided an adequate representation of the vertical response dynamics of a Sea King Mk 50 helicopter in hover was derived. In order to achieve this it was necessary to include blade flapping, inflow and rotor speed dynamics in the model, which then included 28 parameters to be estimated. By fixing and constraining a number of these, as suggested in the previous section, the number of independent parameters was reduced to 14. An identification strategy was developed which enabled excellent matches of vertical acceleration and rotor speed to be achieved, and consistent estimates of most parameters, with the possible exception of parameters associated with the rotor speed, Ω, to be obtained. A particular example for response to a collective pulse is shown in Figure 4. Of particular interest is the region between two and three seconds in the rotor speed records, where relatively large variations in rotor speed are not predicted.

The importance of a proper representation of rotor speed in a vertical acceleration model is illustrated in Figure 5 which shows the effect of neglecting rotor speed dynamics entirely. In this case blade flapping and inflow dynamics are included but with parameters fixed at values based on those derived in Reference 2. Any attempt to extract parameters by matching the acceleration in Figure 5 with a model excluding rotor speed dynamics led to a divergence of the algorithm. Such a model fails entirely to reproduce the second acceleration peak at about 2.5 seconds. While the inclusion of rotor speed dynamics leads to an excellent match for the vertical acceleration, this success is somewhat blunted by the uncertainty in many of the Ω parameters which can vary substantially from case to case, thus detracting from the predictive value of the model.

4.2 Model Derivation

In an attempt to identify a consistent model with good prediction qualities, the importance of including blade lagging dynamics was investigated. A blade lagging model was derived from first principles by balancing the aerodynamic and inertial moments about the lag hinge. Allowing for variations in the coupled blade lagging angle, ζ, blade flapping angle, β, and rotor speed, Ω, the following equation for blade lagging dynamics can be derived

$$\ddot{\zeta} - 2\beta\dot{\beta}\dot{\zeta} + 2\Omega\beta\dot{\beta} - \dot{\Omega}\left(1 + \frac{e\,M_\beta}{I_\beta}\right) + \frac{eM_\beta\zeta\Omega^2}{I_\beta} = \frac{M_{\zeta_A}}{I_\beta} \qquad (2)$$

with I_β and M_β being the blade moment of inertia and moment of mass respectively, about the flap / lag hinge, e is the hinge offset distance and $M_{\zeta A}$ is the aerodynamic lagging moment about the hinge. Similarly, the blade flapping equation is

$$\ddot{\beta} + \Omega^2\left(1 + \frac{eM_\beta}{I_\beta}\right)\beta - 2\beta\dot{\zeta}\Omega - \beta\zeta\dot{\Omega} - \frac{M_\beta\dot{w}}{I_\beta} = \frac{M_{\beta_A}}{I_\beta} \qquad (3)$$

where w is the vertical velocity (positive down) and $M_{\beta A}$ is the aerodynamic flapping moment about the hinge.

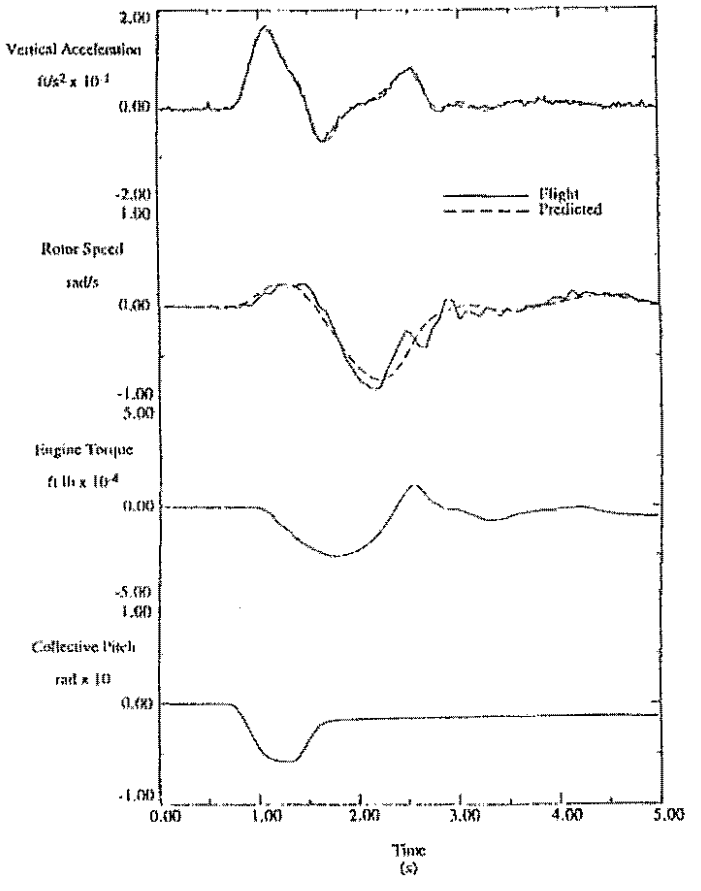

Figure 4 - Matched Acceleration Model

The rotor speed equation has the form

$$I_z\dot{\Omega} - N\Big[2\Omega\left(I_\beta + eM_\beta\right)\beta\dot{\beta} + \left(I_\beta + eM_\beta\right)\ddot{\zeta} - eM_\beta\beta\zeta\ddot{\beta} - eM_\beta\zeta\left(\dot{\beta}^2 + \dot{\zeta}^2\right) - 2\left(I_\beta + eM_\beta\right)\beta\dot{\beta}\dot{\zeta} + 2e\Omega M_\beta\zeta\dot{\zeta}\Big] = Q_E + Q_A \quad (4)$$

where I_z is the total rotor moment of inertia about the shaft, Q_E is the engine torque and Q_A is the total aerodynamic torque about the shaft.

The equations for vertical motion and inflow dynamics remain as before (Reference 2) with the driving force on the right hand side being rotor aerodynamic thrust in both cases. Expressions for the aerodynamic moments, torque, and thrust can be derived using simple strip theory and details can be

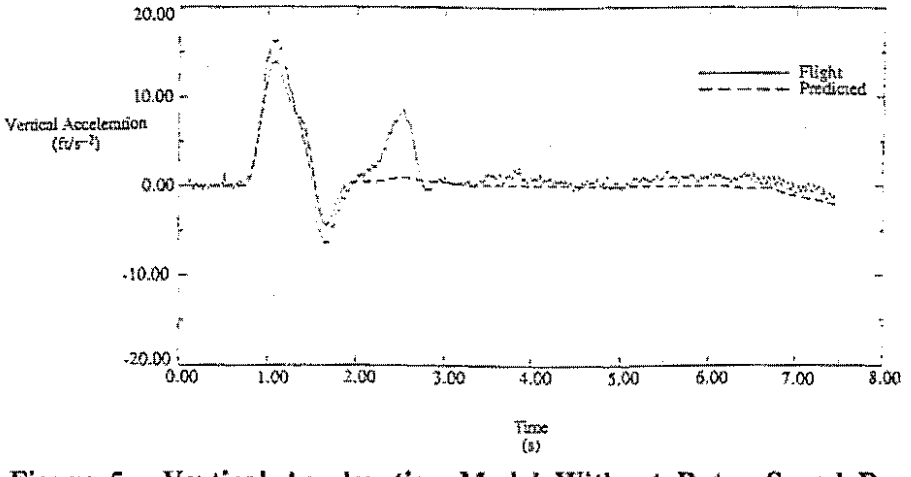

Figure 5 - Vertical Acceleration Model Without Rotor Speed Dynamics

found in Reference 5. Lag aerodynamic damping is of course augmented by a dominant contribution from the lag damper. Linearisation of the equations about a reference state of steady hover with zero vertical velocity leads to a small perturbation model of the form:

$$\begin{bmatrix} 1 & Z_{\ddot{\beta}} & 0 & 0 & 0 & 0 & 0 \\ \beta_{\dot{w}} & 1 & 0 & 0 & 0 & 0 & \beta_{\dot{\Omega}} \\ 0 & 0 & 1 & 0 & 0 & 0 & 0 \\ 0 & 0 & 0 & 1 & 0 & 0 & \zeta_{\dot{\Omega}} \\ 0 & 0 & 0 & 0 & 1 & 0 & 0 \\ 0 & 0 & 0 & 0 & 0 & 1 & \upsilon_{\dot{\Omega}} \\ 0 & \Omega_{\ddot{\beta}} & 0 & \Omega_{\ddot{\zeta}} & 0 & 0 & 1 \end{bmatrix} \begin{bmatrix} \dot{w} \\ \ddot{\beta} \\ \dot{\beta} \\ \ddot{\zeta} \\ \dot{\zeta} \\ \dot{\upsilon} \\ \dot{\Omega} \end{bmatrix} = \begin{bmatrix} Z_w & Z_{\dot{\beta}} & Z_\beta & Z_{\dot{\zeta}} & Z_\zeta & Z_\upsilon & Z_\Omega \\ \beta_w & \beta_{\dot{\beta}} & \beta_\beta & \beta_{\dot{\zeta}} & \beta_\zeta & \beta_\upsilon & \beta_\Omega \\ 0 & 0 & 0 & 0 & 0 & 0 & 0 \\ \zeta_w & \zeta_{\dot{\beta}} & \zeta_\beta & \zeta_{\dot{\zeta}} & \zeta_\zeta & \zeta_\upsilon & \zeta_\Omega \\ 0 & 0 & 0 & 0 & 0 & 0 & 0 \\ \upsilon_w & \upsilon_{\dot{\beta}} & \upsilon_\beta & \upsilon_{\dot{\zeta}} & \upsilon_\zeta & \upsilon_\upsilon & \upsilon_\Omega \\ \Omega_w & \Omega_{\dot{\beta}} & \Omega_\beta & \Omega_{\dot{\zeta}} & \Omega_\zeta & \Omega_\upsilon & \Omega_\Omega \end{bmatrix} \begin{bmatrix} w \\ \dot{\beta} \\ \beta \\ \dot{\zeta} \\ \zeta \\ \upsilon \\ \Omega \end{bmatrix}$$

$$+ \begin{bmatrix} Z_\theta & 0 \\ \beta_\theta & 0 \\ 0 & 0 \\ \zeta_\theta & 0 \\ 0 & 0 \\ \upsilon_\theta & 0 \\ \Omega_\theta & \Omega_Q \end{bmatrix} \begin{bmatrix} \theta_C \\ Q_E \end{bmatrix} \qquad (5)$$

The total number of parameters in Equation 5 is now 47, compared to the previous 28. A priori expressions for these parameters (Reference 5) indicate a number of possible constraints which can be applied to the new parameters. For example, the ζ derivatives (w_ζ, β_ζ, υ_ζ, Ω_ζ) can be constrained to equal the respective θ derivative (w_θ, β_θ, υ_θ, Ω_θ) multiplied by a factor of $-K_2$, the flap lag coupling. However there is no simple relationship for the $\dot{\zeta}$ derivatives. Other parameters such as the $\dot{\Omega}$ derivatives ($\beta_{\dot{\Omega}}$, $\zeta_{\dot{\Omega}}$, and $\upsilon_{\dot{\Omega}}$) can be taken to be small and their values fixed. Yet other parameters are sufficiently uncertain in value so that no conclusion as to their importance can be reached. On the other hand it is clear that parameters such as ζ_ζ, related to the lag frequency, and $\zeta_{\dot{\zeta}}$, the lag damping, are key parameters which need to be allowed to vary. Similarly some freedom must be allowed to parameters such as ζ_Ω, ζ_w, etc. which determine the extent of cross coupling between modes.

4.3 Results

Even following the principles discussed above, it was not possible to reduce the number of parameters sufficiently to enable a simultaneous match of both vertical acceleration and rotor speed time histories. However it was possible to decouple the problem, first by fixing the z, β, and υ derivatives at either a priori values or values based on the results of Reference 2, and matching only the Ω record. The results for seven identified parameters are summarised in Table 1, together with an indication of accuracy in brackets, given by the Cramer - Rao bound multiplied by a factor of 10. Secondly using these values as a guide for the Ω and ζ parameters, the vertical acceleration record was matched and eight z, β, and υ derivatives estimated. The results are given in Table 2. The large Cramer - Rao bounds for some of the parameters e.g. Z_Ω and υ_Ω in Table 2 indicate that almost no confidence can be placed in these identified values.

Table 1 – Parameters for Ω Match

Parameter	A Priori Value	Identified Value	
Ω_Ω	-1.28	-0.97	(0.38)
Ω_θ	-40.0	-45.3	(8.0)
Ω_Q	0.000093	0.00012	(0.00001)
Ω_ζ	0.68	3.2	(2.2)
ζ_ζ	-7.0	-3.6	(2.3)
ζ_ζ	-38.0	-46.7	(16.9)
ζ_θ	45.0	47.2	(26.4)

Bracketed values are Cramer - Rao Bounds x 10

Table 2 – Parameters for ẇ Match

Parameter	A Priori Value	Identified Value	
Z_w	-1.034	-1.50	(0.40)
Z_Ω	-4.6	2.5	(7.3)
Z_θ	-441.0	-480.9	(70.5)
β_β	-253.0	-509.1	(459)
β_θ	284.0	387.2	(538)
υ_w	6.8	6.0	(3.9)
υ_Ω	12.95	-19.7	(39.5)
υ_θ	1250	1065	(696)

Bracketed values are Cramer - Rao Bounds x 10

The equivalent time history matches are shown in Figure 6. It is clear that there is room for some improvement. In fact the vertical acceleration match is not as good as obtained in Figure 4 with the simpler model. However the Ω match in Figure 6 demonstrates the improvement achieved by including lag, especially in the ability to reproduce the peaks at about 2.5 and 3 seconds. It could be anticipated that for a manoeuvre more violent than the present half 'g' vertical acceleration peak, these effects would be more pronounced and consequently more important to represent accurately.

Finally, the main conclusion from the parameter results in Tables 1 and 2 is that additional information, such as blade flapping angle and / or blade lagging angle measurements, would be highly

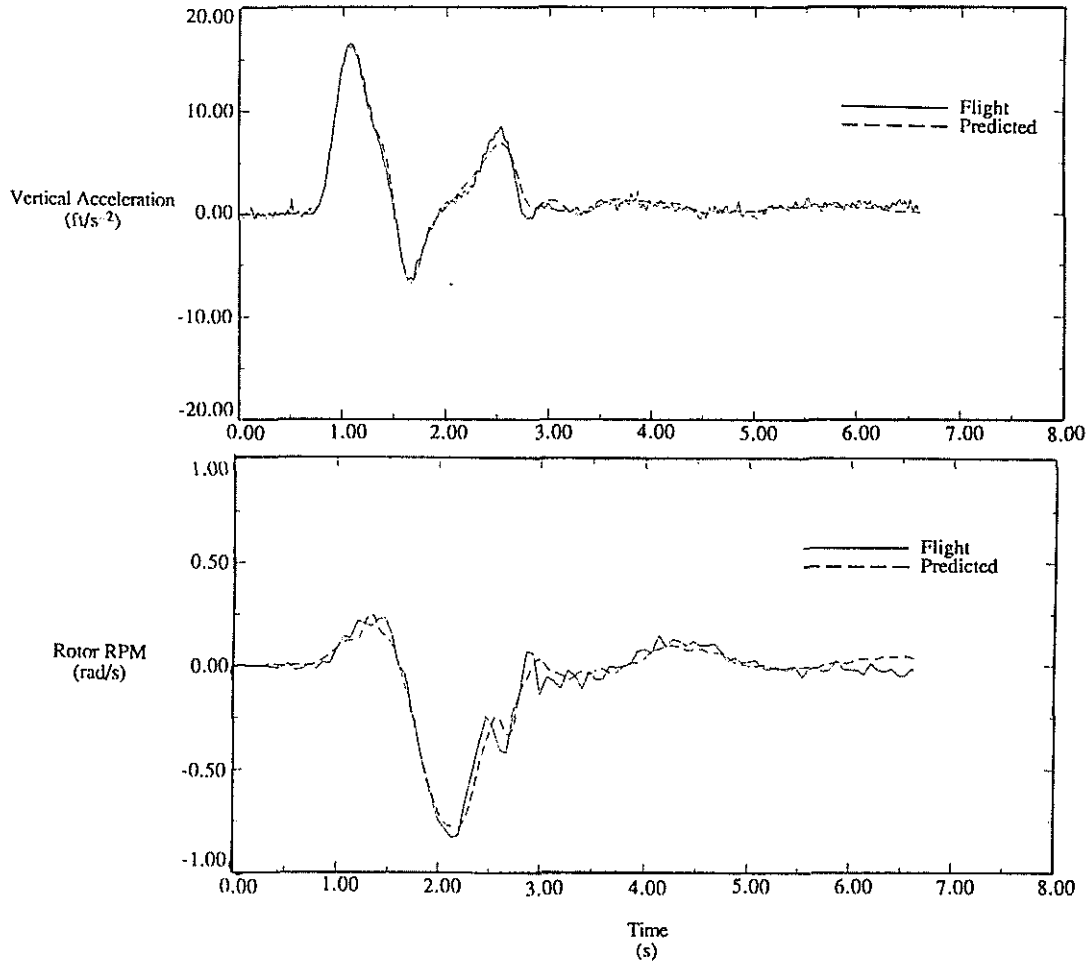

Figure 6 - Matched Vertical Acceleration Model Including Blade Lagging Dynamics

desirable if a consistent model with good predictive properties is required. The relatively large Cramer - Rao bounds on many parameters indicate low confidence in the present values. Additional data would allow some of the present constraints to be eased, thus leading to better time fits and consequently smaller confidence bands on the identified model parameters.

5. CYCLIC RESPONSE

5.1 Background

In Section 2 the inability to predict the cross coupled roll response to a longitudinal stick input was illustrated. The aim in this section is to identify an adequate model which can consistently predict both primary and cross coupled responses to a cyclic stick input. In order to sharpen our focus, the first step has been to limit the model to a hovering situation, for which Sea King flight data is available. This results in a number of simplifications in the equations due to a zero advance ratio. It is further assumed that u, v, and w velocities remain negligible throughout the manoeuvre and that yaw rate is also small throughout. This can be verified by reference to the flight measurements such as those shown in Figure 3 for u and v. For cyclic stick inputs it can also be shown that, under these conditions, rotor thrust can be taken to be constant and that blade coning angle, a_0, and mean inflow υ_o, do not change. These simplifications mean that attention can be focused on pitch and roll responses to cyclic stick inputs taking into account the effects of sine and cosine components of blade flapping (b_1, a_1) and dynamic inflow (υ_S, υ_C). While the Maximum Likelihood algorithm used here is not restricted to linear models,the relatively small excursions in all variables allow derivation of a small perturbation model, which can facilitate interpretation of the results.

5.2 Model Derivation

The rolling and pitching equations with respect to a set of body axes fixed in the helicopter, and with origin at the centre of gravity, can be written

$$I_X \dot{p} - I_{ZX}\, pq \approx I_X \dot{p} = L \tag{6}$$

$$I_Y \dot{q} + I_{ZX}\, p^2 \approx I_Y \dot{q} = M \tag{7}$$

where p and q are the pitch and roll rates, L and M are the rolling and pitching moments and I_X, and I_Y are the moments of inertia. The terms involving the product of inertia I_{ZX} are taken to be negligible. L and M consist of rotor hub moment components and components due to moments of the hub side and drag forces (Y_F and H_F) about the helicopter centre of gravity, and for zero shaft tilt are represented by

$$L = L_H + Y_F\, h_F \tag{8}$$

$$M = M_H + H_F\, h_F \tag{9}$$

where h_F is the distance of the hub above the centre of gravity. Expressions for L_H, M_H, Y_F, and H_F can be found in Reference 6, which includes blade flapping but not dynamic inflow terms. For example, the change in rolling moment due to cyclic stick input is approximated by

$$\Delta L_H = -C_1\left(\ddot{b}_1 - 2\Omega\dot{a}_1 - \Omega^2 b_1\right) + C_2\left(B_1 - K_1 b_1 - \frac{p}{\Omega} - \frac{\dot{b}_1}{\Omega} + a_1\right) \tag{10}$$

where C_1 and C_2 are constants depending on blade geometry and mass characteristics and B_1 is the sine component of control input, which is generally represented as

$$\theta = \theta_{COLL} - A_1 \cos\psi - B_1 \sin\psi \tag{11}$$

and a_1 and b_1 are components of blade flapping given by

$$\beta = a_0 - a_1 \cos\psi - b_1 \sin\psi \tag{12}$$

Tip path plane equations for a_1 and b_1 are given in Reference 7. For example, the equation for a_1 (again neglecting inflow dynamics) for zero advance ratio is

$$\ddot{a}_1 + \gamma\Omega\dot{a}_1\left(\frac{1}{8} - \frac{\varepsilon}{3}\right) + 2\Omega\dot{b}_1 + \Omega^2\left(P^2 - 1\right)a_1 + \gamma\Omega^2\left(\frac{1}{8} - \frac{\varepsilon}{3}\right)b_1$$
$$= \gamma\Omega^2\left(\frac{1}{8} - \frac{\varepsilon}{6}\right)A_1 - 2\Omega\left(1 + \frac{eM_\beta}{I_\beta}\right)p - \dot{q} - \gamma\Omega\left(\frac{1}{8} - \frac{\varepsilon}{6}\right)q \tag{13}$$

where γ is the Lock number ε is the ratio of the hinge offset to rotor radius e/R, and P is a constant depending on blade characteristics.

For inflow dynamics the small perturbation model described in References 8 and 9 is used. In particular for inflow represented as

$$\upsilon(r, \psi) = \upsilon_0 + \upsilon_s \frac{r}{R}\sin\psi + \upsilon_c \frac{r}{R}\cos\psi \tag{14}$$

the relevant equations for υ_s and υ_c are

$$M_{22}\dot{\upsilon}_s + \frac{\Omega}{L_{22}}\upsilon_s = \Omega^2 R\,\Delta C_{L_A} \tag{15}$$

$$M_{33}\dot{\upsilon}_c + \frac{\Omega}{L_{33}}\upsilon_c = \Omega^2 R\,\Delta C_{M_A} \tag{16}$$

where

$$M_{22} = M_{33} = -16/45\pi$$

$$L_{22} = L_{33} = -\Omega R/\upsilon_o$$

and ΔC_{L_A} and ΔC_{M_A} are perturbations in the aerodynamic rolling and pitching moments on the rotor disk. To obtain expressions for these we follow the approach outlined in Reference 10, which relates the aerodynamic moments to rotor motions. This results in the equations

$$\Delta C_{L_A} = -C_4\left[\frac{\ddot{b}_1}{\Omega^2} + \frac{eM_\beta}{I_\beta}b_1 - \frac{2}{\Omega}\left(1 + \frac{eM_\beta}{I_\beta}\right)q + \frac{\dot{p}}{\Omega^2} - \frac{2}{\Omega}\dot{a}_1\right] \tag{17}$$

$$\Delta C_{M_A} = -C_4\left[\frac{\ddot{a}_1}{\Omega^2} + \frac{eM_\beta}{I_\beta}a_1 + \frac{2}{\Omega}\left(1 + \frac{eM_\beta}{I_\beta}\right)p + \frac{\dot{q}}{\Omega^2} + \frac{2}{\Omega}\dot{b}_1\right] \tag{18}$$

where C_4 is a constant depending on blade characteristics. Finally, to incorporate dynamic inflow in the rolling, pitching, and blade flapping equations the aerodynamic terms involving p and q in those equations should be modified by replacing p with $(p - \upsilon_s/R)$ and q with $(q - \upsilon_c/R)$. This includes the p term in Equation 10 and the q term in Equation 13. In the latter equation, the p and $\dot{q}$ terms relate to the coriolis and body accelerations and hence are not modified.

Equations 6 to 18 constitute a complete set for prediction of roll and pitch responses to cyclic stick inputs in hover. Linearisation about a reference state of steady hover leads to a small perturbation model of the form:

$$
\begin{bmatrix}
I_X & 0 & 0 & 0 & 0 & C_1 & 0 & 0 \\
0 & I_Y & 0 & 0 & C_1 & 0 & 0 & 0 \\
0 & 0 & 1 & 0 & 0 & 0 & 0 & 0 \\
0 & 0 & 0 & 1 & 0 & 0 & 0 & 0 \\
0 & 1 & 0 & 0 & 1 & 0 & 0 & 0 \\
1 & 0 & 0 & 0 & 0 & 1 & 0 & 0 \\
0 & \frac{C_4}{\Omega^2} & 0 & 0 & \frac{C_4}{\Omega^2} & 0 & \frac{M_{22}}{\Omega^2 R} & 0 \\
\frac{C_4}{\Omega^2} & 0 & 0 & 0 & 0 & \frac{C_4}{\Omega^2} & 0 & \frac{M_{22}}{\Omega^2 R}
\end{bmatrix}
\begin{bmatrix}
\dot{p} \\ \dot{q} \\ \dot{a}_1 \\ \dot{b}_1 \\ \ddot{a}_1 \\ \ddot{b}_1 \\ \dot{\upsilon}_C \\ \dot{\upsilon}_S
\end{bmatrix} =
$$

$$
\begin{bmatrix}
L_p & L_q & L_{a_1} & L_{b_1} & L_{\dot{a}_1} & L_{\dot{b}_1} & L_{\upsilon_C} & L_{\upsilon_S} \\
M_p & M_q & M_{a_1} & M_{b_1} & M_{\dot{a}_1} & M_{\dot{b}_1} & M_{\upsilon_C} & M_{\upsilon_S} \\
0 & 0 & 0 & 0 & 1 & 0 & 0 & 0 \\
0 & 0 & 0 & 0 & 0 & 1 & 0 & 0 \\
a_p & a_q & a_{a_1} & a_{b_1} & a_{\dot{a}_1} & a_{\dot{b}_1} & a_{\upsilon_C} & a_{\upsilon_S} \\
b_p & b_q & b_{a_1} & b_{b_1} & b_{\dot{a}_1} & b_{\dot{b}_1} & b_{\upsilon_C} & b_{\upsilon_S} \\
\upsilon_{C_p} & 0 & \upsilon_{C_{a_1}} & 0 & 0 & \upsilon_{C_{\dot{b}_1}} & \upsilon_{C_{\upsilon_C}} & 0 \\
0 & \upsilon_{S_q} & 0 & \upsilon_{S_{b_1}} & \upsilon_{S_{\dot{a}_1}} & 0 & 0 & \upsilon_{S_{\upsilon_S}}
\end{bmatrix}
\begin{bmatrix}
p \\ q \\ a_1 \\ b_1 \\ \dot{a}_1 \\ \dot{b}_1 \\ \upsilon_C \\ \upsilon_S
\end{bmatrix} +
\begin{bmatrix}
L_{A_1} & L_{B_1} \\
M_{A_1} & M_{B_1} \\
0 & 0 \\
0 & 0 \\
a_{A_1} & 0 \\
0 & b_{B_1} \\
0 & 0 \\
0 & 0
\end{bmatrix}
\begin{bmatrix}
A_1 \\ B_1
\end{bmatrix}
\tag{19}
$$

A priori expressions for the elements of the matrices in Equation 19 are given in Appendix A. Because of the symmetry in the hover situation the a priori expressions indicate that the total number of independent parameters is actually half that shown in Equation 19. The number can be reduced even further by noting that many parameters differ from one another only by simple multiplicative factors. For example $a_{\dot{a}_1}$ and a_{b_1} differ only by a factor of Ω. Similarly, L_{B_1} and L_{υ_s} differ by a factor of ΩR. On the other hand, the expressions for L_p, M_q, and L_q, M_p do not take into account fuselage aerodynamic effects which introduce an asymmetry not present in the rotor alone (see Figure 1). For this reason symmetry constraints are relaxed in the results that follow, for the parameters where asymmetric aerodynamic effects may be significant. The final model has 23 independent parameters.

5.3 Steady State Analysis of Blade Flapping and Inflow Variations

To investigate the likely effect of including blade flapping and inflow variations, the values of the pitch and roll derivatives, L_p, L_q, L_{A_1}, L_{B_1}, M_p, M_q, M_{A_1}, and M_{B_1}, can be examined. Their values, as given in Appendix A, contain no effects due to flapping or inflow, since these effects are contained within their respective derivatives (L_{a_1} etc). However, by looking at steady state values of flapping and inflow, *effective values* for the pitch and roll derivatives can be obtained and compared with the actual derivatives above.

5.3.1 Blade Flapping

Taking steady state values for flapping parameters, (ie. $\dot{a}_1 = \dot{b}_1 = 0$), and neglecting inflow changes entirely (ie. $\upsilon_c = \upsilon_s = 0$), the top two rows of Equation (19) reduce to

$$I_x \dot{p} = L_p p + L_q q + L_{a_1} a_{1_{ss}} + L_{b_1} b_{1_{ss}} + L_{A_1} A_1 + L_{B_1} B_1 \tag{20}$$

$$I_y \dot{q} = M_p p + M_q q + M_{a_1} a_{1_{ss}} + M_{b_1} b_{1_{ss}} + M_{A_1} A_1 + M_{B_1} B_1 \tag{21}$$

Steady state expressions for the flapping parameters, $(a_1, b_1)_{ss}$, as functions of p, q, A_1 and B_1, can be calculated from Equation (13) and its b_1 counterpart with $\dot{a}_1 = \dot{b}_1 = 0$. Substituting in Equations (20) and (21) results in the equivalent rigid body model

$$I_x \dot{p} = L'_p p + L'_q q + L'_{A_1} A_1 + L'_{B_1} B_1 \tag{22}$$

$$I_y \dot{q} = M'_p p + M'_q q + M'_{A_1} A_1 + M'_{B_1} B_1 \tag{23}$$

where L'_p, L'_q etc. are the *effective* derivatives and incorporate the effects of steady state flapping. For example, L'_p is given by

$$L'_p = L_p + AL_{a_1} + BL_{b_1} \tag{24}$$

where

$$A = \frac{(L_{b_1} - I_x b_{b_1})(I_y a_p - M_p) - (M_{b_1} - I_y a_{b_1})(I_x b_p - L_p)}{(M_{b_1} - I_y a_{b_1})(I_x b_{a_1} - L_{a_1}) - (L_{b_1} - I_x b_{b_1})(I_y a_{a_1} - M_{a_1})} \tag{25}$$

$$B = \frac{1}{(L_{b_1} - I_x b_{b_1})} \left[I_x b_p - L_p + A\,(I_x b_{a_1} - L_{a_1}) \right] \tag{26}$$

5.3.2 Inflow and Flapping

Taking steady state values for υ_c and υ_s, (ie. $\dot{\upsilon}_C = \dot{\upsilon}_S = 0$), as well as steady state values of a_1 and b_1, the top two rows of Equation (19) reduce to

$$I_x \dot{p} = L_p p + L_q q + L_{a_1} a_{1_{ss}} + L_{b_1} b_{1_{ss}} + L_{\upsilon_c} \upsilon_{c_{ss}} + L_{\upsilon_s} \upsilon_{s_{ss}} + L_{A_1} A_1 + L_{B_1} B_1 \tag{27}$$

$$I_y \dot{q} = M_p p + M_q q + M_{a_1} a_{1_{ss}} + M_{b_1} b_{1_{ss}} + M_{\upsilon_c} \upsilon_{c_{ss}} + M_{\upsilon_s} \upsilon_{s_{ss}} + M_{A_1} A_1 + M_{B_1} B_1 \tag{28}$$

Steady state expressions for a_1, b_1, υ_c and υ_s as functions of p, q, A_1 and B_1, can be calculated simultaneously from Equations (13) (and its b_1 counterpart), (15) and (16) with $\dot{a}_1 = \dot{b}_1 = \dot{\upsilon}_C = \dot{\upsilon}_S = 0$.

Substituting in Equations (27) and (28) results in the equivalent model

$$I_x \dot{p} = L''_p p + L''_q q + L''_{A_1} A_1 + L''_{B_1} B_1 \tag{29}$$

$$I_y \dot{q} = M''_p p + M''_q q + M''_{A_1} A_1 + M''_{B_1} B_1 \tag{30}$$

where L''_p, L''_q etc. are the *effective* derivatives and incorporate the effects of steady state blade flapping and inflow changes. Values for the eight derivatives are listed in Table 3 and are discussed next.

Table 3 – Values for Pitch and Roll Derivatives

Derivative	Rigid Body Components only	With Flapping	With Flapping and Inflow
$L_p = M_q$	-10511	-7976	-13370
$L_q = -M_p$	-1486	-23907	-34827
$L_{A_1} = -M_{B_1}$	91425	186220	194973
$L_{B_1} = M_{A_1}$	230220	12457	15982

5.3.3 Discussion

Control Derivatives (L_{A_1}, L_{B_1}, M_{A_1}, M_{B_1})

The effect of flapping terms in the $\dot{p}$, $\dot{q}$ equations approximately doubles the direct derivatives L_{A_1}, M_{B_1} and has an overwhelming effect on the cross derivatives L_{B_1}, M_{A_1} by reducing their magnitude by approximately 17 times. Adding the inflow terms makes little difference to the direct derivatives but increases cross derivatives by approximately 30%.

Damping Derivatives (L_p, L_q, M_p, M_q)

The effect of flapping terms in the $\dot{p}$, $\dot{q}$ equations causes a small reduction of approximately 24% in the magnitude of the direct derivatives L_p, M_q, but increases the magnitude of the cross derivatives L_q, M_p by approximately 16 times. Adding the dynamic inflow terms increases direct derivative magnitudes by about 67% while increasing the cross derivative magnitudes by a further 45%.

The preceding analysis demonstrates the importance of accounting for blade flapping and inflow changes in a cyclic response model. The flapping contributions have a substantial effect on the primary response, as expected, and are a dominant factor in the cross-coupled response. The effects of inflow variations, while not as important as flapping, are seen to be significant for both primary and cross-coupled responses, and hence should not be neglected.

The steady state blade flapping and inflow analysis presented here results in equivalent rigid body models, but does not account for the transient effects of blade flapping and inflow dynamics. These are addressed in the following section.

5.4 Results

Two sets of flight data were available, both representing the response to a longitudinal cyclic pulse in hover. The control inputs are shown in Figures 7(a) and 8(a), one a fore cyclic pulse (Flight 1) and one an aft cyclic pulse (Flight 2). The resultant roll and pitch rates, p and q, are shown by the solid lines in Figures 7(b) - (e) and 8(b) - (e). Note the non zero value of p at zero time in Figure 8 - this was due to the helicopter being not quite trimmed in roll before the start of the cyclic manoeuvre.

The maximum Likelihood procedure was used to estimate parameters for models of varying complexity. The predicted responses are shown by the dashed lines in Figures 7(b) - (e) and 8(b) - (e).

Results were first obtained using a rigid body model with 6 independent parameters L_p, L_q, L_{B_1}, M_p, M_q, M_{B_1}, and are shown in Figures 7(b) and 8(b). The direct response, q, is modelled reasonably well however the cross response p is modelled very badly in both cases.

As a first improvement, the simple rigid model can be retained and unknown time shifts in p and q can be added resulting in 8 independent parameters. Results are shown in Figures 7(c) and 8(c). Both p and q show an improved match however there is still ample room for further improvement in the cross response p. In particular, while the first peak in p is now fairly well matched, there is no representation of subsequent peaks. It is shown next that inclusion of blade dynamics is required to accurately model the cross response.

Including blade flapping results in a model with 34 unknown parameters which after applying constraints was reduced to 16 unknowns. Results are shown in Figures 7(d) and 8(d). Most noticeable is the large improvement in fit for the cross response, p, and also a slight improvement in the fit of q, as predicted in Section 5.3.

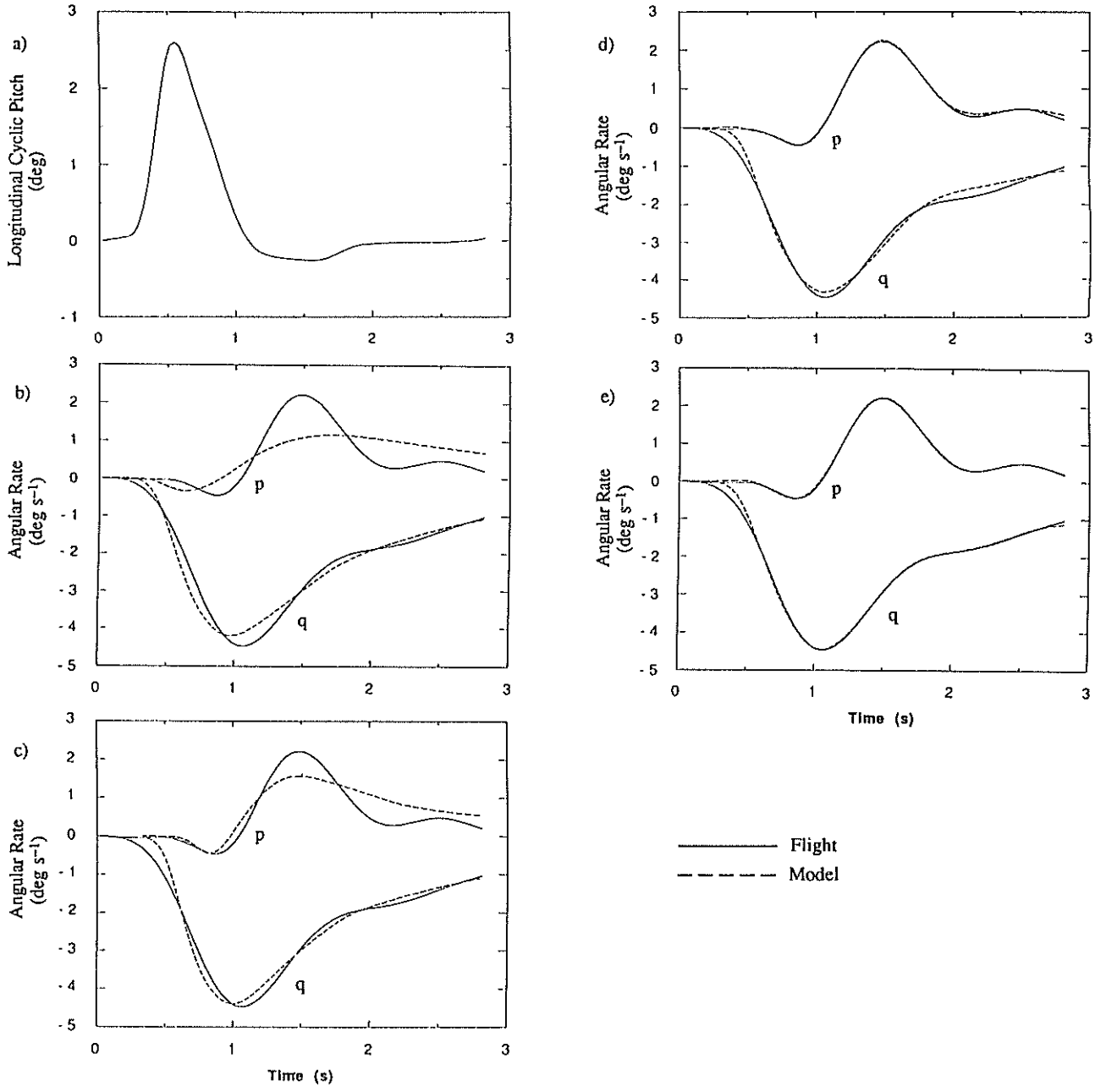

Figure 7 - Roll and Pitch Response to Longitudinal Cyclic Pitch Pulse (Flight 1) a) Control Input, b)-e) Identified Response for Various Models (See Text)

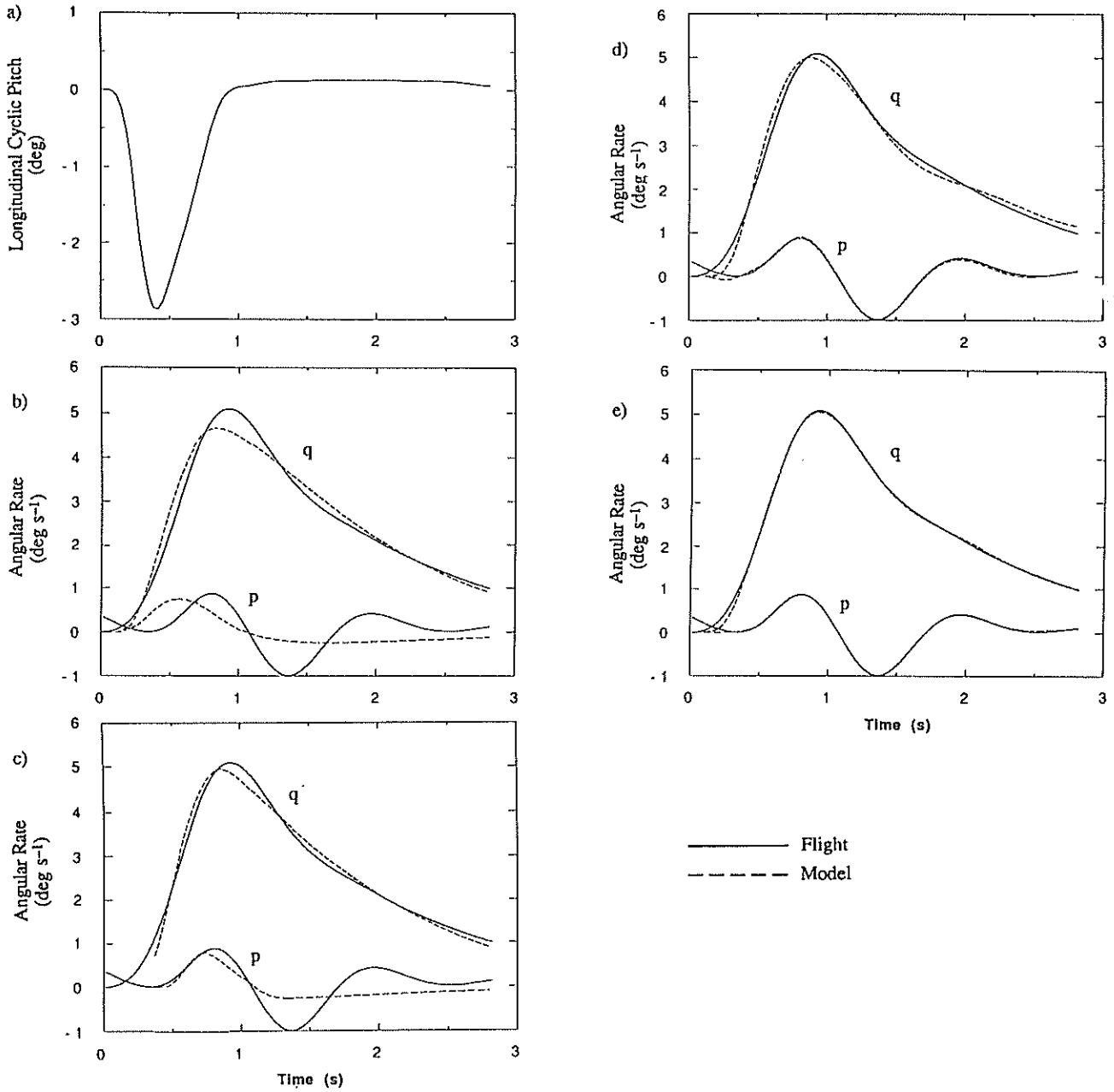

Figure 8 - Roll and Pitch Response to Longitudinal Cyclic Pitch Pulse (Flight 2)
a) Control Input, b)-e) Identified Response for Various Models (See Text)

Table 4 - Identified Parameters for Various Models (Flight 1)

Parameter	A Priori Value	Identified Value			
		Rigid Body Model	With Time Shifts	With Flapping	With Flapping & Dynamic Inflow
L_p	−10511	−19610 (12640)	−121300 (32200)	−5230 (490)	−9780 (10230)
L_q	−1486	−8560 (6030)	−49060 (22230)	26070 (2290)	5174 (3740)
$L_{a_1}=-M_{b_1}$	218779	-	-	274100 (11260)	195500 (10920)
$L_{b_1}=M_{a_1}$	3305	-	-	269700 (10840)	90700 (11700)
$L_{\dot{a}_1}=-M_{\dot{b}_1}$	−1529	-	-	59070 (2680)	16550 (3130)
$L_{\dot{b}_1}=M_{\dot{a}_1}$	−10329	-	-	−30720 (3320)	−36450 (2900)
L_{υ_c}	102.6	-	-	-	26.8 (93)
$L_{\upsilon_s}=M_{\upsilon_c}$	343.7	-	-	-	311.0 (70)
$L_{A_1}=-M_{B_1}$	91425	205200 (30120)	371700 (60700)	−41420 (70660)	−12450 (63720)
$L_{B_1}=M_{A_1}$	230220	−12840 (20350)	−60290 (38070)	*held fixed*	203700 (15250)
M_p	1486	18790 (38420)	−218400 (71030)	180800 (59300)	47320 (44700)
M_q	−10511	$=L_p$	$=L_p$	−4404 (19450)	−32620 (18000)
M_{υ_s}	−102.6	-	-	-	245 (152)
$a_p=-b_q$	−45.7	-	-	0.83 (5)	26.2 (23)
$a_q=b_p$	−26.0	-	-	−10.9 (1.2)	−40.9 (3.2)
$a_{a_1}=b_{b_1}$	−66.2	-	-	−100.0 (4)	−271.7 (22)
$a_{b_1}=-b_{a_1}$	−542.6	-	-	−144.3 (6)	−416.5 (47)
$a_{\dot{a}_1}=b_{\dot{b}_1}$	−24.8	-	-	−27.6 (1.3)	−104.0 (8)
$a_{\dot{b}_1}=-b_{\dot{a}_1}$	−43.8	-	-	3.61 (1.1)	49.7 (8)
$a_{\upsilon_c}=b_{\upsilon_s}$	0.839	-	-	-	1.19 (0.3)
$\upsilon_{c_p}=-\upsilon_{s_q}$	−0.0027	-	-	-	*held fixed*
$\upsilon_{c_{a_1}}=\upsilon_{s_{b_1}}$	−0.00124	-	-	-	*held fixed*
$\upsilon_{c_{\dot{b}_1}}=-\upsilon_{s_{\dot{a}_1}}$	−0.0026	-	-	-	*held fixed*
$\upsilon_{c_{\upsilon_c}}=\upsilon_{s_{\upsilon_s}}$	−0.000085	-	-	-	−0.00006 (0.00001)
$M_{22}/(\Omega^2 R)$	0.0000076	-	-	-	0.0000097 (0.000004)
I_y	46325	*held fixed*	*held fixed*	127300 (24000)	73790 (19900)
τ_p	0.0	-	0.283 (0.18)	-	-
τ_q	0.0	-	0.10 (0.04)	-	-

Bracketed values are Cramer - Rao Bounds x 10

Finally, the combined blade flapping and dynamic inflow model discussed in Section 5.2 was implemented. Due to the large number of unknown parameters (23 after applying constraints), the parameter estimation procedure was applied in two stages. Firstly, the dynamic inflow parameters were held fixed, as were parameters I_y and a_{υ_c}, while L_{B_1} and M_q were constrained to be $-\Omega L_p$ and L_p respectively. This reduced the number of unknowns to 14, and then using the estimated parameter results from this run as a priori results for a second run, the full complement of 23 parameters was allowed to vary. Results (Figures 7(e) and 8(e)) show further improvement in both p and q, particularly q, as predicted in Section 5.3. Both variables are matched almost perfectly. There is however a discrepancy early on in q in both flight tests, the cause of which is unknown.

Table 5 - Identified Parameters for Various Models (Flight 2)

Parameter	A Priori Value	Identified Value			
		Rigid Body Model	With Time Shifts	With Flapping	With Flapping & Dynamic Inflow
L_p	−10511	−44720 (47830)	−712100 (81400)	−6847 (1900)	−5957 (38600)
L_q	−1486	−2847 (5000)	−39880 (53240)	35450 (7960)	24260 (12140)
$L_{a_1}=-M_{b1}$	218779	-	-	261700 (30700)	216900 (38700)
$L_{b_1}=M_{a1}$	3305	-	-	272700 (34000)	93710 (35700)
$L_{\dot{a}_1}=-M_{\dot{b}_1}$	−1529	-	-	58020 (7430)	18690 (9500)
$L_{\dot{b}_1}=M_{\dot{a}_1}$	−10329	-	-	−28230 (6300)	−37480 (8500)
L_{υ_c}	102.6	-	-	-	−71.1 (190)
$L_{\upsilon_s}=M_{\upsilon_c}$	343.7	-	-	-	318.7 (200)
$L_{A_1}=-M_{B_1}$	91425	167400 (39900)	227800 (23860)	−250600 (71430)	43450 (66940)
$L_{B_1}=M_{A_1}$	230220	−20930 (23830)	−226200 (76550)	*held fixed*	151900 (44170)
M_p	1486	145100 (71600)	$=-L_q$	166000 (68450)	90890 (55400)
M_q	−10511	−18640 (15060)	−26640 (7000)	−34630 (21410)	−27160 (26400)
M_{υ_s}	−102.6	-	-	-	415 (350)
$a_p=-b_q$	−45.7	-	-	−8.61 (7)	−19.2 (31)
$a_q=b_p$	−26.0	-	-	−13.4 (3)	−25.6 (6.6)
$a_{a_1}=b_{b_1}$	−66.2	-	-	−83.7 (12)	−201.1 (48)
$a_{b_1}=-b_{a_1}$	−542.6	-	-	−139.5 (19)	−200.0 (66)
$a_{\dot{a}_1}=b_{\dot{b}_1}$	−24.8	-	-	−27.2 (3)	−72.9 (16)
$a_{\dot{b}_1}=-b_{\dot{a}_1}$	−43.8	-	-	1.68 (2)	44.2 (18)
$a_{\upsilon_c}=b_{\upsilon_s}$	0.839	-	-	-	1.11 (0.4)
$\upsilon_{c_p}=-\upsilon_{s_q}$	−0.0027	-	-	-	*held fixed*
$\upsilon_{c_{a1}}=\upsilon_{s_{b1}}$	−0.00124	-	-	-	*held fixed*
$\upsilon_{c_{\dot{b}1}}=-\upsilon_{s_{\dot{a}1}}$	−0.0026	-	-	-	*held fixed*
$\upsilon_{c_{\upsilon c}}=\upsilon_{s_{\upsilon s}}$	−0.000085	-	-	-	−0.000051 (0.00002)
$M_{22}/(\Omega^2 R)$	0.0000076	-	-	-	0.0000064 (0.000004)
I_y	46325	*held fixed*	*held fixed*	92990 (31700)	98450 (28640)
τ_p	0.0	-	0.333 (0.22)	-	-
τ_q	0.0	-	0.083 (0.03)	-	-

Bracketed values are Cramer - Rao Bounds x 10

Parameter values for the above 4 models are given in Tables 4 and 5, together with an indication of error in brackets, given by the Cramer - Rao bound multiplied by a factor of 10. In most cases, the parameter values are in approximate agreement for the two flight tests, if the possible errors in brackets are taken into account. For the equivalent rigid body model, with and without time shifts, the identified parameters should be compared with those in Table 3. The poor agreement reflects the inadequate predictive qualities of such an approach. Nevertheless, the consistent estimated time shift values may provide useful information for handling qualities purposes.

For the full model, the identified parameters are broadly in line with the a priori values in most cases, noting also that a priori estimates for some parameters e.g. L_{b_1}, $L_{\dot{a}_1}$, L_{υ_c}, are very sensitive to small changes in reference trim values. One exception is L_q which also varies widely between the two flights. This may reflect the non-linear aerodynamic rotor / tail interactions which would be expected to produce different results since one flight is predominantly a pitch down manoeuvre while the other is a

pitch up. Another parameter, $a_{\dot{b}_1}$, appears to be reasonably well identified but differs in sign from the a priori estimate, suggesting a possible error in model derivation which needs closer examination.

6. CONCLUDING REMARKS

The use of a time domain maximum likelihood identification program for general non-linear systems has been demonstrated in the investigation of rotor dynamic effects apparent in Sea King helicopter flight data. Models have been developed including blade flapping and inflow dynamics, for response to cyclic inputs, plus rotor speed and blade lagging dynamics for collective response manoeuvres. For the latter, the importance of representing rotor speed transients has been discussed and the effects of lagging effects on rotor speed records illustrated.

For cyclic response, a systematic study showing the need to include higher order effects to obtain good time history matches has been reported, although a rigid body model structure can be used to obtain information on response time delays.

The large number of parameters in both cyclic and collective response models has necessitated making full use of a priori expressions to minimise the number of parameters to be identified, and the development of a staged approach in order to ensure convergence of the algorithm. The availability of additional, more optimal, flight data would alleviate this problem. Taking into account the estimated error bounds, the identified parameters have been shown to be in reasonable agreement, despite some notable exceptions, with a priori predictions.

REFERENCES

1. M.J. Williams and A.M. Arney, Validation of the ARL Mathematical Model of the Sea King Mk 50 Helicopter. *ARL Aero Tech Memo 383*, November 1986
2. R.A. Feik and R.H. Perrin, Identification of an Adequate Model for Collective Response Dynamics of a Sea King Helicopter in Hover. *ARL Aero Tech Memo 399*, July 1988 (to appear in Vertica)
3. R.E. Maine and K.W. Iliff, Application of Parameter Estimation to Aircraft Stability and Control - The Output Error Approach. *NASA RP - 1168*, 1986
4. J. Blackwell, A Maximum Likelihood Parameter Estimation Program for General Non-linear Systems. *ARL Aero Tech Memo 392*, January 1988
5. R.H. Perrin and R.A. Feik, Derivation of Helicopter Vertical Response Equations in Hover. *ARL Flight Mechanics Tech Memo* (In Publication)
6. R.T.N. Chen, A Simplified Rotor System Mathematical Model for Piloted Flight Dynamics Simulation. *NASA TM 78575*, May 1979
7. R.T.N. Chen, Effects of Primary Rotor Parameters on Flapping Dynamics. *NASA TP 1431*, January 1980
8. G.H. Goankar and D.A. Peters, Effectiveness of Current Dynamic - Inflow models in Hover and Forward Flight. *Journal of the American Helicopter Society*, Vol. 31, No. 2, April 1986
9. D.A. Peters and H. HaQuang, Technical Note : Dynamic Inflow for Practical Applications. *Journal of the American Helicopter Society*, Vol. 33, No. 4, October 1988
10. J.C. Wang, P.D. Talbot, and D. Tran, An Analytical Approach to the Determination of Dynamic Inflow Coefficients in Helicopter Forward Flight. *Proceedings of the HTP - 6 Workshop on Parameter Identification*, (Edited by P.C. Tarttelin and G.D. Padfield), RAE FM WP(88) 067, November 1988

APPENDIX A – A Priori Expressions for Cyclic Response Model

Parameter	A Priori Expression	Calculated Value (Sea King)
$L_p = M_q$	$-\frac{C_2}{\Omega} - \frac{C_3 h_F a_0}{6\Omega}$	–10 511
$L_q = -M_p$	$\frac{C_3 h_F}{\Omega}\left[\frac{1}{6}(\theta_0 - K_1 a_0) + \frac{\theta_T}{8} - \frac{\bar{\upsilon}_0}{2}\right]$	–1 486
$L_{a_1} = -M_{b_1}$	$C_2 + C_3 h_F\left[a_0\left(\frac{1}{6} - \frac{\varepsilon}{4}\right) - \frac{K_1 \bar{\upsilon}_0}{4}\right]$	218 779
$L_{b_1} = M_{a_1}$	$C_1\Omega^2 - C_2 K_1 + C_3 h_F\left[(\theta_0 - K_1 a_0)\left(\frac{1}{3} - \frac{\varepsilon}{4}\right) - \theta_T\left(\frac{\varepsilon}{6} - \frac{1}{4}\right) - \frac{K_1 a_0}{6} - \frac{3\bar{\upsilon}_0}{4}\right]$	3 305
$L_{a_1} = -M_{b_1}$	$2\Omega C_1 + \frac{C_3 h_F}{\Omega}\left[(\theta_0 - K_1 a_0)\left(\frac{1}{6} - \frac{\varepsilon}{4}\right) - \theta_T\left(\frac{\varepsilon}{6} - \frac{1}{8}\right) - \frac{\bar{\upsilon}_0}{2}\right]$	–1 529
$L_{b_1} = M_{a_1}$	$-\frac{C_2}{\Omega} - \frac{C_3 h_F}{\Omega}\left(\frac{1}{6} - \frac{\varepsilon}{4}\right)a_0$	–10 329
$L_{\upsilon_C} = -M_{\upsilon_s}$	$-\frac{C_3 h_F}{\Omega R}\left[\frac{1}{6}(\theta_0 - K_1 a_0) + \frac{\theta_T}{8} - \frac{\bar{\upsilon}_0}{2}\right]$	102.6
$L_{\upsilon_s} = M_{\upsilon_C}$	$\frac{C_2}{\Omega R} + \frac{C_3 h_F a_0}{6\Omega R}$	343.7
$L_{A_1} = -M_{B_1}$	$\frac{C_3 h_F \bar{\upsilon}_0}{4}$	91 425
$L_{B_1} = M_{A_1}$	$C_2 + \frac{C_3 h_F a_0}{6}$	230 220
$a_p = -b_q$	$-2\Omega\left(1 + \frac{eM_\beta}{I_\beta}\right)$	–45.7
$a_q = b_p$	$-\frac{\gamma\Omega}{2}\left(\frac{1}{4} - \frac{\varepsilon}{3}\right)$	–26.0
$a_{a_1} = b_{b_1}$	$-\Omega^2\left(P^2 - 1\right)$	–66.2
$a_{b_1} = -b_{a_1}$	$-\gamma\Omega^2\left(\frac{1}{8} - \frac{\varepsilon}{3}\right)$	–542.6
$a_{\dot{a}_1} = b_{\dot{b}_1}$	$-\gamma\Omega\left(\frac{1}{8} - \frac{\varepsilon}{3}\right)$	–24.8
$a_{\dot{b}_1} = -b_{\dot{a}_1}$	-2Ω	–43.8
$a_{\upsilon_C} = b_{\upsilon_s}$	$\frac{\gamma\Omega}{2R}\left(\frac{1}{4} - \frac{\varepsilon}{3}\right)$	0.839
$a_{A_1} = b_{B_1}$	$\frac{\gamma\Omega^2}{2}\left(\frac{1}{4} - \frac{\varepsilon}{3}\right)$	569.4
$\upsilon_{C_p} = -\upsilon_{S_q}$	$\frac{-2C_4}{\Omega}\left(1 + \frac{eM_\beta}{I_\beta}\right)$	–0.002 7
$\upsilon_{C_{a1}} = \upsilon_{S_{b1}}$	$-C_4\frac{eM_\beta}{I_\beta}$	–0.001 24
$\upsilon_{C_{\dot{b}1}} = -\upsilon_{S_{\dot{a}1}}$	$\frac{-2C_4}{\Omega}$	–0.002 6
$\upsilon_{C_{\upsilon_C}} = \upsilon_{S_{\upsilon_s}}$	$\frac{-1}{\Omega R L_{22}}$	–0.000 085
C_1	$\frac{eNM_\beta}{2g}$	7.63
C_2	$\frac{R\varepsilon C_3}{6}$	150 436
C_3	$\frac{N}{2}\rho a c R(\Omega R)^2$	859 636
C_4	$\frac{a\sigma}{2\gamma}$	0.028
$P^2 - 1$	$\frac{eM_\beta}{I_\beta} + \frac{\gamma K_1}{8}\left(1 - \frac{4\varepsilon}{3}\right)$	0.139